

ESS LOW ENERGY BEAM TRANSPORT TUNING DURING THE FIRST BEAM COMMISSIONING STAGE

R. Miyamoto*, C. S. Derrez, E. Laface, Y. Levinsen, N. Milas, A. G. Sosa, R. Tarkeshian
 C. Thomas, ESS, Lund, Sweden

Abstract

Beam commissioning of the ion source (IS) and low energy beam transport (LEBT) of the European Spallation Source is ongoing on its site as of writing this paper and continues until June 2019. The LEBT consists of two solenoids with integrated dipole correctors to steer, focus, and match the high current divergent beam out of the IS to the following radio frequency quadrupole (RFQ). It is also equipped with a suite of diagnostics devices to provide a full characterization of the beam for achieving a good transport within the LEBT, optimizing the matching to the RFQ, and also providing references to numerical simulations. This paper presents results of beam characterization campaign from the ongoing beam commissioning period, including the matching at the RFQ interface based on emittance sampling for varied strengths of the solenoids and verification of the linear model for the trajectory and beam envelope.

INTRODUCTION

The European Spallation Source, under construction in Lund, Sweden, will be a spallation neutron source driven by a superconducting proton linac with a design beam power of 5 MW [1]. Beam commissioning (BC) of the linac started from ion source (IS) and following low energy beam transport (LEBT) section in September 2018 and is scheduled to continue until June 2019. Overall status of the IS and LEBT as well as characterization of the IS is presented in [2]. This paper presents results of the LEBT BC, focusing on characterization of its linear optics and matching to the following radio frequency quadrupole (RFQ) section.

IS AND LEBT OVERVIEW

This section provides brief overviews over the IS and LEBT of ESS. The IS and LEBT were in-kind contributions of INFN-LNS and tested with beam on their site prior to delivery to the ESS site [3–6]. The IS of ESS is a microwave discharge source and produces a high quality proton beam with current up to ~ 80 mA at 75 keV. The beam out of the IS includes small fraction of other ion species, mainly H_2^+ and H_3^+ , and proton fraction is typically around 85% [7]. Nominal beam pulse length and repetition rate of ESS Linac are 2.86 ms and 14 Hz, making duty cycle 4%, but we typically extract a ~ 6 ms pulse from the IS. The initial part of the pulse, generated during the stabilization period of the IS, is removed by a chopper in the LEBT. Beam parameters out of the IS are listed in Table 1 together with those at the target.

* ryoichi.miyamoto@ess.se

Table 1: High-level Beam Parameters at IS and Target

Parameter	Units	IS	Target
Average power	kW	~ 0.5	5000
Kinetic energy	MeV	0.075	2000
Peak current (total)	mA	~ 85	62.5
Peak current (proton)	mA	~ 70	62.5
Pulse length	ms	~ 6	2.86
Pulse repetition rate	Hz	14	14
Duty cycle	%	~ 8	4

Figure 1 shows a LEBT schematic. It is ~ 2.5 m long and consisting of two focusing solenoids, a tank (*Permanent Tank*) housing diagnostics devices and the chopper, and an iris for adjusting beam current. Each solenoid also houses coils to form dipole correctors (*steerers*) for each transverse plane. The last component is a collimator with an aperture radius of 7 mm at its end. During this BC period, another tank (*Commissioning Tank*) is placed in the position of the RFQ and allows to house additional diagnostics devices.

Five types of diagnostics devices are included in the LEBT, and their details and deployment statuses are summarized in [8]. For current measurement, there are two beam current monitors (BCMs) and one Faraday cup (FC). The FC can be placed in either of the tanks. Beam induced fluorescence monitors (BIFMs) provides centroid position and one dimensional profile of the beam. A pair for each transverse plane is in Permanent Tank, and another pair in Commissioning Tank is currently under deployment. Each tank houses one Allison scanner type emittance measurement unit (EMU), both for the vertical plane, allowing to measure emittance and Courant-Snyder (CS) parameters at two locations in the beam-line. Doppler detector provides information of the fractions of ion species as well as their energies but has not yet been deployed on the ESS site. In this paper, we mainly show beam characterizations based on the BIFM and EMU.

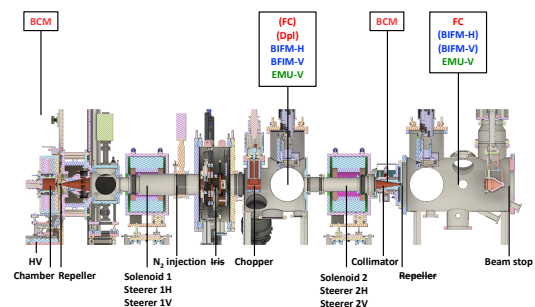


Figure 1: ESS LEBT schematic.

Table 2: LEBT Magnets Settings for the Two IS Settings (*Standard* and *Low*) with Beam Parameters Out of the LEBT

Parameter	Units	Standard	Low
IS current	mA	87	58
Solenoid 1	mT	257	256
Solenoid 2	mT	216	228
Steerer 1H	mT	-0.34	-0.34
Steerer 1V	mT	0.49	0.22
Steerer 2H	mT	-0.85	-0.51
Steerer 2V	mT	0	0.78
Current	mA	71	51
Emittance	π mm mrad	0.38	0.26

In [2], beam characterizations were presented for two IS settings, each referred to as *Standard Setting* and *Low (Current) Setting*. This paper also presents characterizations of the beams from these two IS settings, but focuses are on measurements with the BIFMs and EMU in Commissioning Tank. Table 2 summarizes settings of the LEBT magnets for each IS setting, which were found by manual scans to maximize the LEBT output current. Note that the listed field values are for the peaks, and the effective lengths of the solenoids, horizontal steerer, and vertical steerer are 284 mm, 157 mm, and 164 mm, for each.

LINEAR OPTICS

Prior to perform detailed beam characterizations, we checked planes and polarities of all the LEBT magnets. For the solenoids, polarities were checked with direct field measurements. For the first set of steerers, the centroid position was recorded with the BIFMs in Permanent Tank during scans of these steerers. The result was compared with the online model [9], and we found the planes of the steerers were swapped. For the second set, while keeping Solenoid 2 off, the LEBT output current was intentionally reduced by producing a horizontal or vertical bump at the RFQ interface, and attempts were made to recover the output current with each steerer. After this exercise, we again found that the planes were swapped and the polarity of the vertical one (after corrected to the right plane) had a wrong polarity.

Beam centroid position measurements of the BIFMs allow standard linear optics diagnostics even at this part of

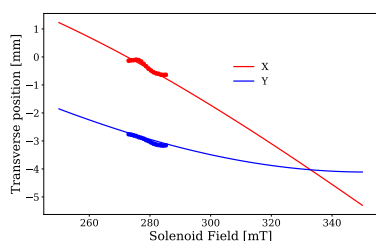


Figure 2: Beam centroid positions at the BIFMs during a Solenoid 1 scan. (Dots: data points and lines: model fits.)

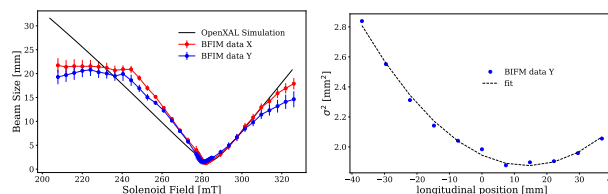


Figure 3: Left: RMS sizes for a Solenoid 1 scan and its model fit. Right: Direct beam waist observation by a BIFM, together with a parabolic fit.

the machine. When the centroid position is measured near the image point of a lens and its strength is scanned, we can acquire information of error sources as fit parameters of a model. In our case, the lens is Solenoid 1, and the error sources are solenoids tilts and the initial trajectory errors out of the IS. Solenoids offsets are negligible compared to the other two, as long as they are within alignment tolerances of 100 to 200 μm . Figure 2 shows the centroid positions measured by the BIFMs (in Permanent Tank) during a scan of Solenoid 1. During the measurement, the IS and LEBT were in Standard Setting. The best model fit was obtained for a Solenoid 1 tilt of -2 mrad around the vertical axis and an initial vertical angle error of 5 mrad. A similar diagnosis will be repeated for Solenoid 2 once the BIFMs in Commissioning Tank become available. The full result of the beam based alignment of the LEBT will be presented in [10].

Beam RMS size measurements with the BIFM allows the conventional *quad scan* technique to reconstruct emittance and CS parameters [11]. Figure 3 (left) shows the measured RMS sizes during a scan of Solenoid 1 with a model fit. The IS and LEBT were in Standard Setting, and the emittance from the model fit was 0.42π mm mrad. When the same measurement was repeated for Low Setting, the measured emittance was 0.29π mm mrad. Note that an emittance value reconstructed this way is sensitive against assumptions in the model such as the initial beam parameters and level of the space charge compensation (SCC). The viewport of the BIFM has a longitudinal size of ~ 80 mm, which is large enough to capture the image of the beam going through a waist. Figure 3 (right) shows the measured squared RMS sizes for eleven slices over the length of the BIFM's measurement range. We can see that the waist is located around 15 mm, where the reference is the center of the device. Emittance is given as a fit parameter of a parabolic fit, and was 0.39π mm mrad. As presented in [2], the direct emittance measurement with the EMU in Permanent Tank showed 0.40π mm mrad for Standard Setting and 0.31π mm mrad for Low Setting. Thus, three different emittance measurement methods are in reasonable agreement.

MATCHING TO RFQ

The standard technique to match the beam to the RFQ is to scan the solenoids and find the settings to maximize transmission through the RFQ. For a typical RFQ, such a condition also almost coincides with that for the best emit-

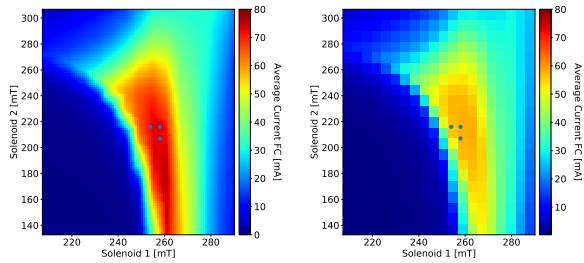


Figure 4: LEBT output current (FC) versus solenoids scan for Standard Setting (left) and Low Setting (right). EMU measurements are shown for the three marked points in Fig. 5.

tance preservation, and this is also the case for the RFQ of ESS [12–15]. As seen in [4], the pattern of the LEBT output current during the solenoids scans could also provide indirect information of the IS output beam as well as the SCC level. Figure 4 shows the measured LEBT output current during the solenoids scan. The current measurement is from the FC in Commissioning Tank, and each value was mean over the plateau (~3 mA). Compared to the most recent simulation [15], a high transmission region is smaller, especially in a region with higher values of Solenoid 2. A large initial divergence, large emittance, and lower SCC level could cause such a trend, but we have not yet been able to find a good set of simulation conditions for TraceWin [16], which allow to reconstruct well those measurements in Fig. 4 [15].

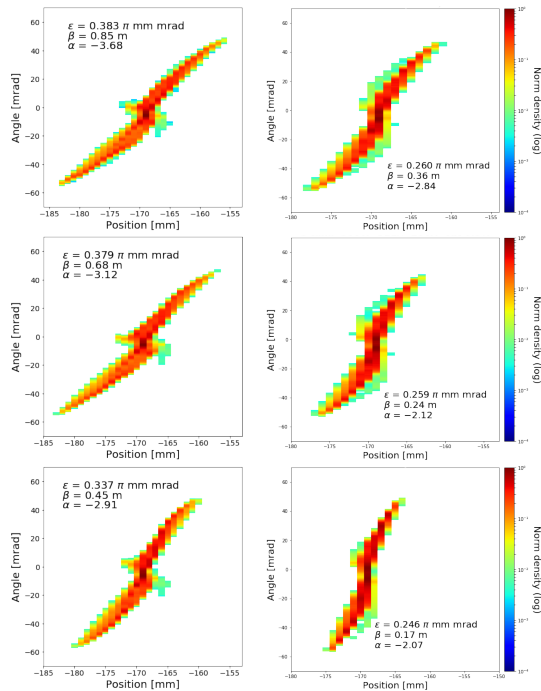


Figure 5: EMU measurements (Commissioning Tank) for Standard Setting (left column) and Low Setting (right column). From top to bottom, strengths of the two solenoids were (258, 216) mT, (258, 207) mT, and (254, 216) mT.

Table 3: Emittance and Estimated Mismatch at the RFQ Interface versus Solenoids Strengths

IS setting	Solenoids [mT]	Emittance [π mm mrad]	Mismatch [%]
Standard	(258, 216)	0.38	211
	(258, 207)	0.38	172
	(254, 216)	0.34	91
Low	(258, 216)	0.26	55
	(258, 207)	0.26	22
	(254, 216)	0.25	21

For both settings of the IS and LEBT in Table 2, we performed EMU measurements in Commissioning Tank. To understand a trend of the matching condition to the RFQ, the measurements were repeated for different sets of solenoids strengths, adjacent to the values in Table 2. As representative cases, we show measurements for three sets in Fig. 5: (258, 216) mT, (258, 207) mT, and (254, 216) mT. Compared to the measurements in Permanent Tank [2], there are ~5% reduction in emittance in Commissioning for Standard Setting and ~15% for Low Setting. Note that the EMUs are currently under deployment processes and thus these measurements are still preliminary. The reduction seen for the third set of the solenoids strengths is however real and due to a small loss of current. Mismatch parameter [17] at the RFQ interface (-149.5 mm upstream of the EMU) was estimated for each EMU measurement by using the simple CS parameters propagation in a drift and ignoring space charge, and the results are summarized in Table 3. As seen in the table, the tested sets of solenoids strengths were not far from the well matched condition for Low Setting, whereas this was not the case for Standard Setting. Note that preparing a good matching directly from the EMU measurement in Commissioning Tank is not at all trivial. The matched condition is not solely determined by the CS parameters, but also depend on current, emittance, and even a distribution shape. In addition, an accurate reconstruction of beam parameters at the RFQ interface requires the level of the SCC, which itself is difficult to measure and simulate especially near a region where the beam size sharply changes.

CONCLUSION

Beam commissioning of the IS and LEBT is ongoing at ESS and will continue until the end of June. This paper presented beam characterization results for the LEBT. The BIFMs proved to be very useful to allow standard linear optics diagnostics and a prompt non-invasive emittance estimation. Preliminary analyses of beam quality and matching condition to the RFQ were performed for two IS settings, and the lower current setting (51 mA out of the LEBT) showed an acceptable levels of emittance and matching condition.

ACKNOWLEDGEMENTS

Authors would like to thank to M. Eshraqi, Gålnander, E. Nilsson, M. Muñoz, and C. Plostinar for useful discussions and their supports on measurements.

REFERENCES

- [1] R. Garoby *et al.*, “The European Spallation Source design”, *Phys. Scr.*, vol. 93, p. 014001, 2018.
- [2] R. Miyamoto *et al.*, “First results of beam commissioning on the ESS site for the ion source and low energy beam transport”, presented at the 10th Int. Particle Accelerator Conf. (IPAC’19), Melbourne, Australia, May 2019, paper MOPTS103, this conference.
- [3] L. Neri *et al.*, “Beam commissioning of the high intensity proton source developed at INFN-LNS for the European Spallation Source”, in *Proc. 8th Int. Particle Accelerator Conf. (IPAC’17)*, Copenhagen, Denmark, May 2017, paper WEOBB2, pp. 2530-2532.
- [4] Ø. Midttun, L. Celona, B. Cheymol, R. Miyamoto, L. Neri, and C. Thomas, “Measurements and simulations of the beam extraction from the ESS proton source”, in *Proc. 17th Int. Conf. on Ion Source*, Geneva, Switzerland, Oct. 2017, p. 080022.
- [5] Ø. Midttun, “Off-site commissioning report for the ESS proton source and LEBT”, ESS, Lund, Sweden, Rep. ESS-0190279, June 2018.
- [6] L. Celona *et al.*, “Ion source and low energy beam transport line final commissioning step and transfer from INFN to ESS”, in *Proc. 9th Int. Particle Accelerator Conf. (IPAC’18)*, Vancouver, Canada, April 2018, paper TUPML073, pp. 1712-1714.
- [7] C. Thomas *et al.*, “Development and commissioning of the Doppler-shift unit for the measurement of the ion species fractions and beam energy of the ESS proton source”, in *Proc. 8th Int. Particle Accelerator Conf. (IPAC’17)*, Copenhagen, Denmark, May 2017, paper MOPVA037, pp. 936-938.
- [8] C. S. Derrez *et al.*, “Initial performance of the beam instrumentation for the ESS IS&LEBT”, presented at the 10th Int. Particle Accelerator Conf. (IPAC’19), Melbourne, Australia, May 2019, paper WEPGW076, this conference.
- [9] N. Milas, S. K. Louisy, and C. Plostinar, “Transverse dynamics and software integration of the ESS low energy beam transport”, in *Proc. 9th Int. Particle Accelerator Conf. (IPAC’18)*, Vancouver, Canada, April 2018, paper TUPAF066, pp. 882-885.
- [10] N. Milas *et al.*, “Beam based alignment of elements and source for the ESS low energy beam transport line,” presented at the 8th Int. Beam Instrumentation Conf. (IBIC’19), Malmö, Sweden, Sept. 2019.
- [11] M. G. Minty and F. Zimmermann, “4.1.1 Single Wire Measurement”, in *Measurement and control of charged particle beams*, Springer-Verlag, Berlin, Heidelberg, 2003, pp. 101-140.
- [12] Y. Levensen *et al.*, “European Spallation Source lattice design status”, in *Proc. 6th Int. Particle Accelerator Conf. (IPAC’15)*, Richmond, Virginia, U.S.A., May 2015, paper THPF092, pp. 3911-3914.
- [13] Y. Levensen, L. Celona, M. Eshraqi, and L. Neri, “In-depth analysis and optimization of the European Spallation Source front end lattice”, in *Proc. 7th Int. Particle Accelerator Conf. (IPAC’16)*, Busan, Korea, May 2016, paper TUPMR020, pp. 1274-1277.
- [14] R. Miyamoto *et al.*, “Preparation towards the ESS linac ion source and LEBT beam commissioning on ESS site”, in *Proc. 9th Int. Particle Accelerator Conf. (IPAC’18)*, Vancouver, Canada, paper TUPAF064, pp. 874-877.
- [15] E. Nilsson, M. Eshraqi, Y. Levensen, and R. Miyamoto, “Beam dynamics simulation with an updated model for the ESS ion source and low energy beam transport”, presented at the 10th Int. Particle Accelerator Conf. (IPAC’19), Melbourne, Australia, May 2019, paper MOPTS083, this conference.
- [16] R. Duperrier, N. Pichoff, and D. Uriot, “Saclay codes review for high intensities linacs computations”, in *Int. Conf. on Computational Sci. (ICCS’02)*, Amsterdam, Netherlands, April 2002, pp. 411-418.
- [17] K. R. Crandall and D. P. Rusthoi, “TRACE 3-D documentation, third edition”, Los Alamos, New Mexico, U.S.A., Rep. LA-UR-90-4146, August 1997.